

Constrained Transport Algorithms for Numerical Relativity.

I. Development of a Finite Difference Scheme

David L. Meier

Jet Propulsion Laboratory, California Institute of Technology, Pasadena, CA 91109

ABSTRACT

A scheme is presented for accurately propagating the gravitational field constraints in finite difference implementations of numerical relativity. The method is based on similar techniques used in astrophysical magnetohydrodynamics and engineering electromagnetics, and has properties of a finite differential calculus on a four-dimensional manifold. It is motivated by the arguments that 1) an evolutionary scheme that naturally satisfies the Bianchi identities will propagate the constraints, and 2) methods in which temporal and spatial derivatives commute will satisfy the Bianchi identities implicitly. The proposed algorithm exactly propagates the constraints in a local Riemann normal coordinate system; *i.e.*, all terms in the Bianchi identities (which all vary as $\partial^3 g$) cancel to machine roundoff accuracy at each time step. In a general coordinate basis, these terms, and those that vary as $\partial g \partial^2 g$, also can be made to cancel, but differences of connection terms, proportional to $(\partial g)^3$, will remain, resulting in a net truncation error. Detailed and complex numerical experiments with four-dimensional staggered grids will be needed to completely examine the stability and convergence properties of this method.

If such techniques are successful for finite difference implementations of numerical relativity, other implementations, such as finite element (and eventually pseudo-spectral) techniques, might benefit from schemes that use four-dimensional grids and that have temporal and spatial derivatives that commute.

Subject headings: relativity: numerical — black holes

1. Introduction

The quest for solutions of dynamical strong gravity problems, such as black hole formation or mergers and gamma-ray burst production, that are astrophysically relevant and accurate enough to predict gravitational wave forms, has occupied much of the last half of the 20th century and beyond. Its history has been frustrated by the need to address several unforeseen numerical problems, including 1) proper initial data to begin the evolution, 2) the development of coordinate

and physical singularities during the evolution, and 3) the growth of numerical instabilities in the time-dependent solutions. These problems have been dealt with by addressing each in turn with such techniques as 1) elevation of the initial data problem to a complete sub-field; 2) development and analysis of appropriate gauge/slicing conditions that avoid coordinate singularities; 3) excision of black hole centers, inside horizons, to avoid physical singularities; and 4) the use of symmetric/hyperbolic equations to enhance numerical stability.

One of the several remaining problems in this field is that, for some problems and some coordinate systems, the constraint-violating modes will grow exponentially. These eventually overwhelm any solution in only a short period of time ($< 100M$), rendering a long simulation (and the computation of any gravitational wave forms) impossible. For very high-resolution simulations the exponential growth of errors begins early and continues until the errors diverge. On the other hand, for simulations with coarse spatial resolution the errors begin and remain at the truncation level until the much smaller constraint violations grow to a level that exceeds the truncation accuracy. Then the solution joins the general exponential growth seen in the high-resolution simulations, blowing up in much the same manner as in the high-resolution case (Scheel *et al.* 2002). The similar behavior of this error at a variety of mesh spacings indicates that it may be a numerical solution to the discrete equations that are being integrated. Current attempts to solve this problem include adding the constraints as penalty functions to the evolution equations and techniques that re-converge the constraint equations every few time steps.

Constraint propagation is also an issue in the solution of Maxwell’s equations. Techniques for doing so in the fields of astrophysical magnetohydrodynamics (MHD) and electromagnetics of antennas and waves have been in place for decades. These enforce the constraints not just stably, but *to machine accuracy*. Finite difference methods for constraint propagation in astrophysical MHD are known as the Evans-Hawley constrained transport (CT) method (Evans & Hawley 1988) and now are an integral part of publicly used codes, such as ZEUS (Stone & Norman 1992a; Stone & Norman 1992b) and ZEUS-3D (Clarke 1996). In engineering electromagnetics these are known as the Yee algorithm (Yee 1966), and have many variants (De Raedt *et al.* 2002). They all involve building a mesh that is staggered in space, and often in time as well, and then defining appropriate vector and scalar quantities at whole or half mesh points.

While the success of CT for electromagnetics is certainly due in part to the linearity of the physical equations, its ability to maintain accuracy of the solenoidal ($\nabla \cdot \mathbf{B} = 0$) and Coulomb ($\nabla \cdot \mathbf{E} = 4\pi\rho_c$) constraints, to a few parts in 10^{14-15} over tens or hundreds of thousands of time steps, is enticing. If such an algorithm can be found for numerical relativity, it could be as useful as excision and other such proven methods.

In this paper the properties of the electromagnetic CT method (and of spacetime itself) are examined, and a similar method is developed for numerical relativity. It is the thesis of this paper,

and subsequent ones in this series, that CT methods work because they build spacetimes in which the temporal and spatial derivatives commute ($[\partial_0, \partial_i] = O(\epsilon_r)$, where ϵ_r is the machine roundoff error). This naturally enforces the Bianchi identities, and it is those implicit identities that propagate the constraints. This thesis is not fully tested in this first paper on the subject. In fact, it will take some time and numerical effort to verify or refute it. Instead, only the first steps are taken here. It is shown that the proposed CT scheme for NR works exactly in Riemann normal coordinates; in general coordinates most terms also cancel. Detailed numerical simulations in four dimensions will be needed to fully explore the method’s stability properties to see if these conditions are sufficient for stable constraint propagation. If successful, however, similar CT methods should be possible for other implementations of numerical relativity, not just for finite differences.

This paper is intended to be the first in a long series that will culminate in a numerical code that is capable of simulating black hole formation and the gamma-ray burst jet generation and gravitational wave production that is expected to result from such events. These issues are important both for dealing properly with the energetics in the system as well as with the expected observational consequences of the event. In order to treat these problems properly, such a code must be capable of evolving the relativistic gravitational field, as well as the fluid matter flowing within that field *and* the electromagnetic field generated by currents flowing in that matter. Part of achieving this goal will be to present a consistent numerical method, from the relativistic gravitational field to specific issues of stellar mergers and collapse. In this paper we lay the groundwork for generating the time-dependent gravitational field and for evolving the electromagnetic field in that metric. In subsequent papers we will present tests of the constrained transport techniques developed herein, and eventually add the stress-energy due to matter and fluid motion to complete the code. Then, specific astrophysical problems will be addressed. The ultimate aim of this work is to foster a closer relationship between astronomers who *observe* black hole systems and those numerical physicists and astrophysicists who study them *theoretically*.

2. Review of CT for Electromagnetics in Flat Spacetime

2.1. The Evans-Hawley CT Method for MHD

For astrophysical MHD the field equations that are solved are

$$\dot{\mathbf{B}} = -c \nabla \times \mathbf{E} \tag{1}$$

with the solenoidal constraint

$$\nabla \cdot \mathbf{B} = 0 \tag{2}$$

(Additional equations are solved, of course, including the conservation of mass, momentum, and energy; but these are not relevant here.) The Evans-Hawley constrained transport technique satisfies equation (2) on the initial hypersurface, usually to machine accuracy, and then uses a differencing scheme for equation (1) that ensures that equation (2) is satisfied on each subsequent hypersurface to the same level of accuracy as on the first. This is done by staggering the grid in space and time (see Figure 1). At whole time steps the magnetic field vector components are defined normal to, and centered on, grid cube faces. At half time steps the electric vector is defined parallel to, and centered on, cube edges. For the initial conditions the magnetic field is derived from a vector potential

$$\mathbf{B} = \nabla \times \mathbf{A} \quad (3)$$

This vector potential is defined on cube edges at $t = {}^0t$, and for evolutionary computations $\dot{\mathbf{B}} \equiv \partial \mathbf{B} / \partial t$ is defined on cube faces, centered in time between ${}^n\mathbf{B}$ and ${}^{n+1}\mathbf{B}$, *i.e.*, at $t = {}^{n+\frac{1}{2}}t$.

At $t = {}^0t$ we see that the solenoidal constraint is satisfied to machine accuracy by this method. For $\Delta x = \Delta y = \Delta z$ we have, simply,

$$\begin{aligned} \nabla \cdot \mathbf{B} &= {}_+B_x - {}_-B_x + {}_+B_y - {}_-B_y + {}_+B_z - {}_-B_z \\ &= \nabla \cdot \nabla \times \mathbf{A} \\ &= ({}_{++}A_z - {}_{+-}A_z) - ({}_{++}A_y - {}_{+-}A_y) - ({}_{-+}A_z - {}_{--}A_z) + ({}_{-+}A_y - {}_{--}A_y) + \\ &\quad ({}_{++}A_x - {}_{+-}A_x) - ({}_{++}A_z - {}_{-+}A_z) - ({}_{-+}A_x - {}_{--}A_x) + ({}_{+-}A_z - {}_{--}A_z) + \\ &\quad ({}_{++}A_y - {}_{-+}A_y) - ({}_{++}A_x - {}_{-+}A_x) - ({}_{+-}A_y - {}_{--}A_y) + ({}_{+-}A_x - {}_{--}A_x) \\ &= O(\epsilon_r) \end{aligned} \quad (4)$$

where ${}_+B_i$ and ${}_ -B_i$ are components on upper and lower cube i -faces, respectively, and the two pre-appended subscript signs on vector potential components A_j indicate the j^{th} edge at the intersection of the upper and/or lower cube faces with normals in the two spatial dimensions orthogonal to j . Similarly, taking the numerical divergence of equation (1) at ${}^{\frac{1}{2}}t$, we have

$$\nabla \cdot \dot{\mathbf{B}} = -c \nabla \cdot \nabla \times \mathbf{E} = O(\epsilon_r)$$

so, at time $t = {}^1t$ the magnetic field remains divergence-free

$$\nabla \cdot {}^1\mathbf{B} = \nabla \cdot {}^0\mathbf{B} + \Delta t \frac{1}{2} (\nabla \cdot \dot{\mathbf{B}}) = O(\epsilon_r)$$

because it is the sum of two divergence-free fields. The solenoidal constraint is therefore preserved to machine accuracy *specifically because the vector identity $\nabla \cdot \nabla \times \mathbf{E} = 0$ is naturally satisfied by the differencing scheme.*

In the above equations the electric field can be computed by any means, and CT still would be maintained. Ideal MHD codes use Ohm's law with infinite conductivity to relate the fluid velocity and the magnetic field:

$$\mathbf{E} = -\frac{\mathbf{v}}{c} \times \mathbf{B}$$

Some astrophysical codes, like ZEUS and several in Japan, use the method of characteristics to preserve Alfvén waves in the \mathbf{E} update, and so are often called MOC-CT codes. However, it is important to realize that CT results simply from the grid staggering and has nothing to do with the method of characteristics or any other \mathbf{E} update scheme.

2.2. The Yee Algorithm for Electromagnetics

In full electrodynamics two more Maxwell's equations are used to determine the electric field, instead of Ohm's law. In vacuum these are

$$\dot{\mathbf{E}} = c \nabla \times \mathbf{B} - 4\pi\mathbf{J} \quad (5)$$

$$\nabla \cdot \mathbf{E} = 4\pi\rho_c \quad (6)$$

Figure 1 then must be modified to include the new quantities \mathbf{J} (current density), ρ_c (charge density), and ϕ (electric potential). (See Figure 2.) We also add another initial data problem at $t = -\frac{1}{2}t$ that solves equation (6) for \mathbf{E} . If, for the moment, we choose the Coulomb gauge and ignore the vector potential, we have

$$\nabla^2\phi = -4\pi\rho_c$$

$$\mathbf{E} = -\nabla\phi$$

Electric potential and charge density then must be defined at cube corners on half time steps, and current density must be defined on cube edges at whole time steps (same as $\mathit{curl} \mathbf{B}$, \mathbf{A} , and $\dot{\mathbf{E}}$; see Figure 2). In an arbitrary gauge, we will have

$$\mathbf{E} = -\nabla\phi - \frac{1}{c}\dot{\mathbf{A}} \quad (7)$$

indicating that $\dot{\mathbf{A}}$ and \mathbf{E} are co-located. The equations are closed by specifying the evolution of ρ_c and \mathbf{J} , which together must satisfy the conservation of charge

$$\nabla \cdot \mathbf{J} = -\dot{\rho}_c \quad (8)$$

so $\dot{\rho}_c$ must be defined on cell corners at whole time steps. This method of staggering was suggested by Yee almost 40 years ago (Yee 1966).

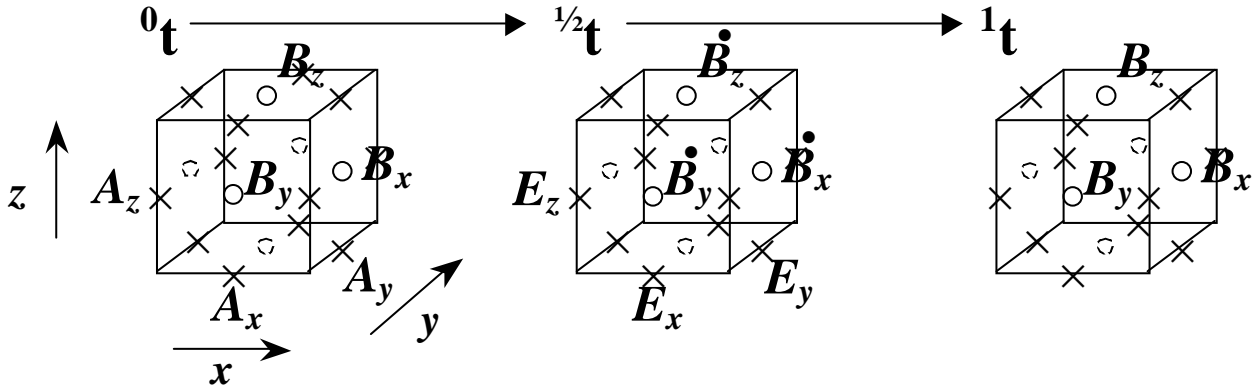


Fig. 1.— Space-time representation for the Evans-Hawley CT scheme. Open circles are face-centered on the cubes and crosses are edge-centered.

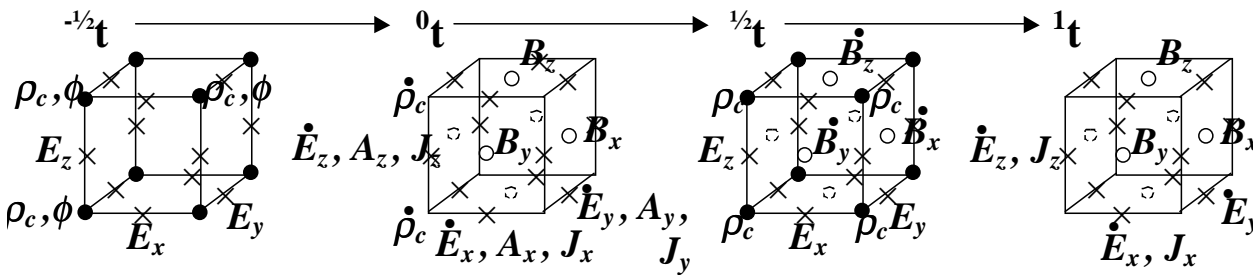


Fig. 2.— Space-time representation for the Yee algorithm. Similar to Figure 1, but with filled circles located at cube corners. Another time step has been added ($-\frac{1}{2}t$, along with electric field quantities).

Constraints are preserved in the Yee algorithm in the same manner as in the Evans-Hawley algorithm. For Faraday’s law and the solenoidal constraint, the procedure is identical. And for Ampere’s law we have

$$\begin{aligned}\nabla \cdot \dot{\mathbf{E}} &= c \nabla \cdot \nabla \times \mathbf{B} - 4\pi \nabla \cdot \mathbf{J} \\ &= O(\epsilon_r) + 4\pi \dot{\rho}_c\end{aligned}$$

which gives the following update for $div \mathbf{E}$:

$$\begin{aligned}\frac{1}{2}(\nabla \cdot \mathbf{E}) &= -\frac{1}{2}(\nabla \cdot \mathbf{E}) + {}^1(\nabla \cdot \dot{\mathbf{E}}) \Delta t \\ &= 4\pi^{-\frac{1}{2}} \rho_c + 4\pi \Delta t {}^1 \dot{\rho}_c + O(\epsilon_r) \\ &= 4\pi^{\frac{1}{2}} \rho_c + O(\epsilon_r)\end{aligned}$$

So the Coulomb constraint is preserved to machine accuracy as long as ρ_c is conserved in the update.

2.3. Covariant formulation of CT for Electrodynamics

Figure 3 re-casts the Yee algorithm in covariant form, using the Faraday tensor \mathbf{F} (instead of the vector fields), the four-current \mathbf{J} , and the vector four-potential \mathbf{A} . This will give important clues to developing a CT scheme for Einstein’s field equations. Maxwell’s equations then become, including constraints,

$$\nabla \cdot \mathbf{M} = 0 \tag{9}$$

$$\nabla \cdot \mathbf{F} = 4\pi \mathbf{J} \tag{10}$$

where $\mathbf{M} \equiv {}^* \mathbf{F}$ is the Maxwell tensor (the dual of \mathbf{F}) and ∇ is now the *four*-gradient operator $\nabla \equiv (\frac{\partial}{\partial t}, \frac{\partial}{\partial x}, \frac{\partial}{\partial y}, \frac{\partial}{\partial z})$. Because \mathbf{M} and \mathbf{F} are antisymmetric, they satisfy tensor identities (analogous

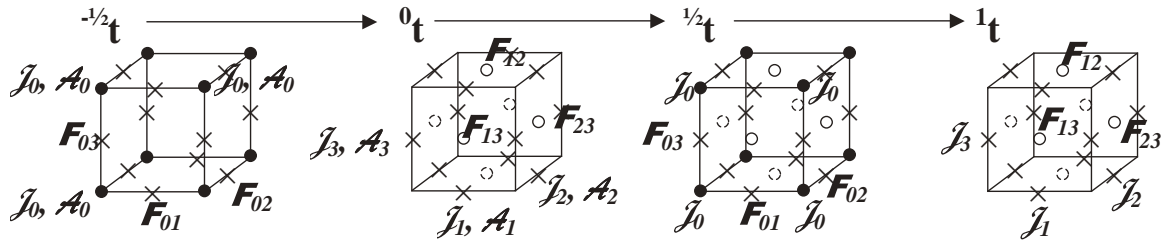


Fig. 3.— Same as Figure 2, but with covariant notation. Note placement of vector components (on hypercube edges) and Faraday tensor components (on hypercube faces).

to the vector identities $\nabla \cdot \nabla \times \mathbf{E}$) called the Bianchi identities

$$\begin{aligned}\nabla \cdot (\nabla \cdot \mathbf{M}) &= 0 \\ \nabla \cdot (\nabla \cdot \mathbf{F}) &= 0\end{aligned}$$

These identities are related to J. A. Wheeler’s classic statement that “the boundary of a boundary is zero”. But, does the staggered grid in Figure 3 automatically satisfy these identities to machine accuracy? A quick analysis of $\nabla \cdot \mathbf{F}$ shows that, in fact, it does. $\nabla \cdot \mathbf{F}$ is a vector that is defined on cell edges at whole time steps and on cell corners at half time steps, and it involves tensor components that are two half-steps away from scalar points (whole time-step cell corners). Taking the divergence of this vector causes like components to cancel, so that

$$\nabla \cdot (\nabla \cdot \mathbf{F}) = O(\varepsilon_r)$$

holds in this differencing scheme.

Because of the zero on the right hand side of equation (9), that equation itself also is often described as a Bianchi identity

$$d\mathbf{F} = 0 \tag{11}$$

where $d\mathbf{F}$ is the differential of the tensor \mathbf{F} , which in component form is given by

$$(d\mathbf{F})_{\alpha\beta\gamma} \equiv F_{[\alpha\beta,\gamma]} = F_{\alpha\beta,\gamma} + F_{\beta\gamma,\alpha} + F_{\gamma\alpha,\beta}$$

where the comma denotes ordinary differentiation ($F_{\alpha\beta,\gamma} \equiv \partial F_{\alpha\beta} / \partial x^\gamma$) and the brackets denote permuted summation.¹ This allows the Faraday tensor to be derived from a vector four-potential

$$\mathbf{F} = d\mathbf{A}$$

or

$$F_{\alpha\beta} = A_{\alpha,\beta} - A_{\beta,\alpha}$$

This is the covariant form for equations (3) and (7). Does the staggered grid automatically enforce $dd\mathbf{A} = 0$ also? Yes. We have already shown this to be the case for the magnetic part (equation 4). For the electric part of $dd\mathbf{A} = 0$ we have

$$\begin{aligned}\nabla \times \mathbf{E} &= -\nabla \times \nabla\phi - \nabla \times \frac{1}{c} \dot{\mathbf{A}} \\ &= \frac{1}{c} \dot{\mathbf{B}} + O(\varepsilon_r)\end{aligned} \tag{12}$$

¹In this paper Greek indices range from 0 to 3, Roman indices i, j, k, \dots range from 1 to 3, and Roman indices a, b, c, \dots will be used to denote a set of three integers with one of the spatial indices missing (*i.e.*, one of the sets $[0, 1, 2]$, $[0, 1, 3]$, or $[0, 2, 3]$).

the second term is $\dot{\mathbf{B}}/c$ to order ϵ_r , and the first term is zero to the same order because of the staggered grid (see the $t = -\frac{1}{2}t$ panel in Figure 2). So equation (12) is just the same Faraday’s law that we are solving to machine accuracy in the spatial part of equation (9) (or equation 1).

To summarize, then, the staggered grid naturally satisfies the Bianchi (and vector) identities in space and time

$$F^{\alpha\beta}{}_{;\beta\alpha} = 0 \quad (13)$$

$$(A_{\alpha,\beta} - A_{\beta,\alpha})_{;\gamma} + (A_{\gamma,\alpha} - A_{\alpha,\gamma})_{;\beta} + (A_{\beta,\gamma} - A_{\gamma,\beta})_{;\alpha} = 0 \quad (14)$$

to machine accuracy for any antisymmetric tensor \mathbf{F} and for any four-vector \mathbf{A} . Here we use the Einstein summation convention, where a repeated index indicates summation over the four coordinates ($F^{\alpha\beta}{}_{;\beta} \equiv \sum_{\beta=0}^3 \partial F^{\alpha\beta} / \partial x^\beta$). Note that equation (13) uses the raised form of \mathbf{F} , but in flat space this involves only multiplying by ± 1 with the Minkowski metric. As a result of this cancellation, when the spatial parts of equations (9) and (10) are integrated forward in time

$$\mathbf{P} \cdot (\nabla \cdot \mathbf{F}) = 4\pi \mathbf{P} \cdot \mathbf{J} \quad \mathbf{P} \cdot (\nabla \cdot \mathbf{M}) = 0$$

(where the spatial projection tensor $P^{\alpha\beta} = n^\alpha n^\beta + g^{\alpha\beta}$ is orthogonal to \mathbf{n}), the time parts (the constraints) are *automatically satisfied to machine accuracy*

$$\mathbf{n} \cdot (\nabla \cdot \mathbf{F}) = 4\pi \mathbf{n} \cdot \mathbf{J} \quad \mathbf{n} \cdot (\nabla \cdot \mathbf{M}) = 0$$

with no additional computation required. *A staggered grid, therefore, has “deep geometric significance”*, because it naturally satisfies the Bianchi identities.

3. CT for Electrodynamics in Curvilinear and Curved Spacetime

CT also works in curvilinear coordinates and in curved spacetime, but the method requires iteration. Again, Maxwell’s equations are

$$\nabla \cdot \mathbf{F} = 4\pi \mathbf{J} \quad d\mathbf{F} = 0$$

but the gradient operator is now the covariant derivative rather than the ordinary derivative

$$F^{\alpha\beta}{}_{;\beta} = 4\pi J^\alpha \quad F_{[\alpha\beta;\gamma]} = 0 \quad (15)$$

where

$$\begin{aligned} T^{\alpha\beta}{}_{;\gamma} &\equiv T^{\alpha\beta}{}_{,\gamma} + \Gamma^\alpha_{\mu\gamma} T^{\mu\beta} + \Gamma^\beta_{\mu\gamma} T^{\alpha\mu} \\ T_{\alpha\beta;\gamma} &\equiv T_{\alpha\beta,\gamma} - \Gamma^\mu_{\alpha\gamma} T_{\mu\beta} - \Gamma^\mu_{\beta\gamma} T_{\alpha\mu} \end{aligned}$$

are the covariant derivatives of a general second-rank tensor \mathbf{T} ,

$$\Gamma^\alpha_{\beta\gamma} \equiv g^{\alpha\mu}\Gamma_{\mu\beta\gamma} \quad (16)$$

$$\Gamma_{\alpha\beta\gamma} \equiv \frac{1}{2}(g_{\alpha\beta,\gamma} + g_{\beta\alpha,\gamma} - g_{\beta\gamma,\alpha}) \quad (17)$$

are different forms of the connection coefficients, and $g^{\alpha\beta}$ is the inverse of the metric $g_{\alpha\beta}$. However, because the Faraday tensor is antisymmetric (as is the Maxwell tensor), equations (15) reduce to

$$F'^{\alpha\beta}_{,\beta} = 4\pi J'^{\alpha} \quad F_{[\alpha\beta,\gamma]} = 0 \quad (18)$$

where

$$F'^{\alpha\beta} \equiv F^{\alpha\beta}\sqrt{-g} \quad J'^{\alpha} \equiv J^{\alpha}\sqrt{-g}$$

and $\sqrt{-g}$ is the volume element (square root of the negative metric determinant). Equations (18) involve only simple differences and known values for the metric. However, unless \mathbf{g} is a diagonal, the raised version of the Faraday tensor $F'^{\alpha\beta}$ involves the sum of several lowered version components at different grid locations

$$F^{\alpha\beta} \equiv g^{\alpha\mu}g^{\beta\nu}F_{\mu\nu}$$

Therefore, the time update of the fundamental variables $F_{\mu\nu}$ will necessarily be implicit, and therefore iterative, as it involves sums over time as well as space.

It is important to realize, however, that even in curvilinear coordinates and curved spacetime, the Bianchi identities

$$F'^{\alpha\beta}_{,\beta\alpha} = 0 \quad (19)$$

will be satisfied to machine accuracy, because $F'^{\alpha\beta}$ is constructed *before* it is differenced and because that differencing is done in precisely the same manner as in equation (13). It does not matter that $F'^{\alpha\beta}$ involves the sum of many tensor components and products of metric components. It only matters that the β and α derivatives commute.

4. A General Finite Difference Prescription for CT for Tensor Field Evolution Problems

Figure 3 suggests the following geometric prescription for a staggered grid when solving covariant tensor field evolution problems. This prescription is depicted schematically in Figure 4, and appears to work for tensors up to at least rank five. The basic rules are

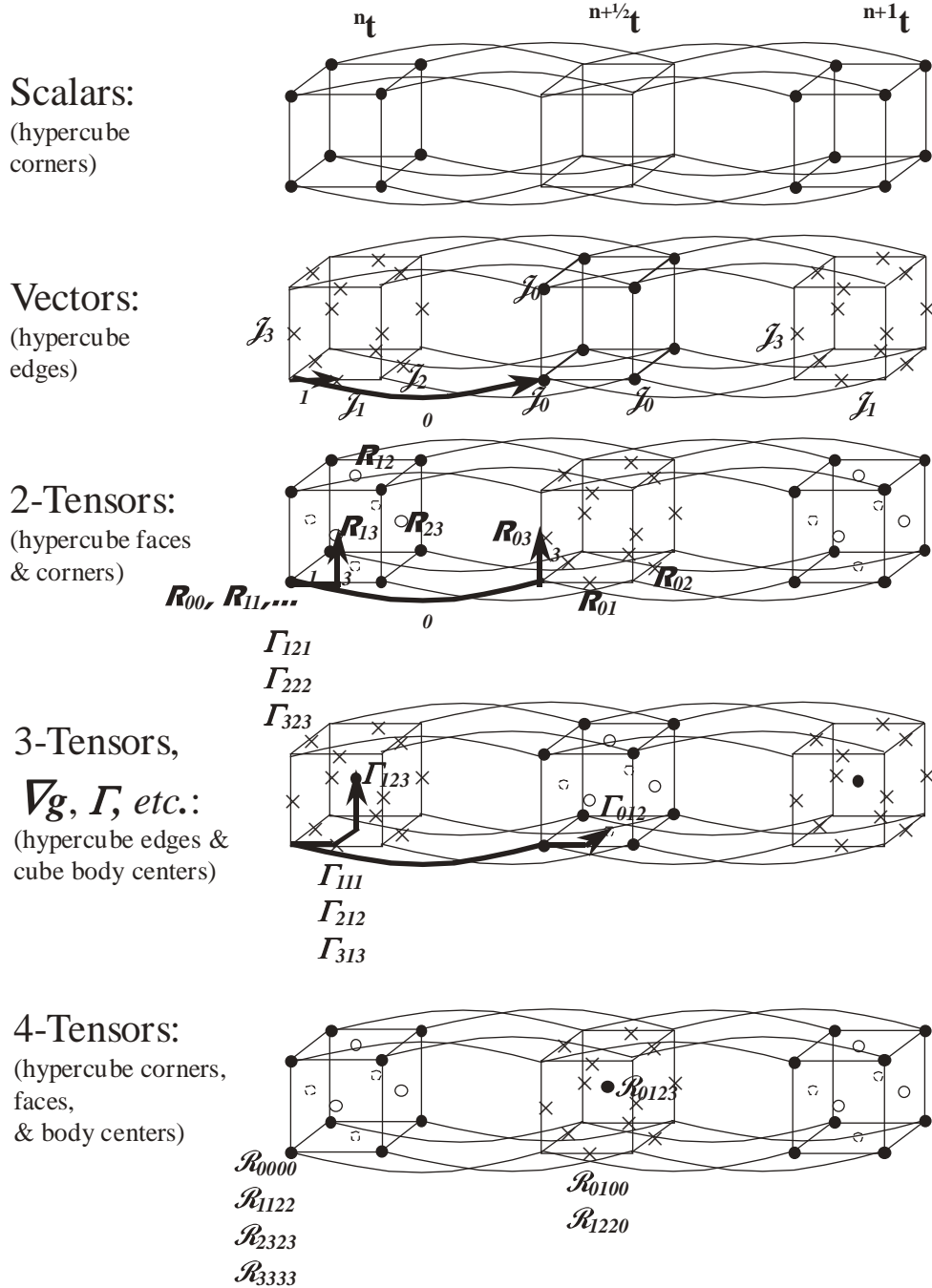


Fig. 4.— Graphical depiction of the four-dimensional staggered grid scheme for different tensor quantities. (See Section 4 for a full description.) The first panel shows filled circles where scalars are located (hypercube corners.) Heavy arrows in the second panel show how to locate the following vector quantities: J_0 (shift one-half step in the 0 dimension); J_1 (shift one-half step in the 1 dimension). The third panel shows how to locate R_{03} by shifting one-half step in the 0 and 3 dimensions, and R_{13} by shifting in the 1 and 3 dimensions. Remaining panels demonstrate third and fourth ranked tensors. Note the hypercube body-center location of R_{0123} .

1. Extend and stagger the grid in time as well as in space. The time extension need not be very deep — only enough cells to compute the tensor components, derivatives, *etc.* to the order of the method. In this paper we use a second order differencing scheme, so we need only one additional half, and one full, time slice.
2. Treat time otherwise like a spatial coordinate. That is, use the same differencing scheme in time as used in space so that temporal and spatial differences commute.
3. Starting at corner nodes on the four-dimensional hypercube cell, define the following quantities in the manner described below. Simply put, a tensor component is located one-half step away from hypercube cell corners in each dimension specified by that component's indices; two repeated indices are equivalent to no shift at all.
 - (a) Scalars: located on 4-cube cell corners (3-cube corners at whole time steps)
 - (b) Vectors: located on 4-cube edges, shifted one-half cell step in the direction specified by that component. That is,
 - i. J^0 on 3-cube cell corners at half time steps
 - ii. J^1 centered on 3-cube x edges at whole time steps
 - iii. J^2 centered on y edges
 - iv. J^3 centered on z edges
 - (c) One-forms: defined like vectors
 - (d) Second-ranked tensors of any type
 - i. $R_{\alpha\alpha}$: defined like scalars, on 3-cube cell corners at whole time steps
 - ii. R_{0j} : centered on 3-cube i -edges at *half* time steps
 - iii. R_{ij} : centered on ij faces at whole time steps
 - (e) Third-ranked tensors and connection coefficients
 - i. $\Gamma_{\alpha\alpha\beta}, \Gamma_{\alpha\beta\alpha}, \Gamma_{\beta\alpha\alpha}$: defined like J^β
 - ii. $\Gamma_{0ij}, \Gamma_{i0j}, \Gamma_{ij0}$: centered on 3-cube ij -faces at half time steps
 - iii. Γ_{ijk} : 3-cube-centered at whole time steps
 - (f) Fourth-ranked tensors
 - i. $R_{\alpha\alpha\beta\gamma}$: defined like $R_{\beta\gamma}$
 - ii. $R_{\alpha\beta\gamma\delta}$ ($\alpha \neq \beta \neq \gamma \neq \delta$): located at 4-cube body centers
 - (g) Bianchi identities: defined like third-ranked tensors (at least one index must be repeated). Examples are $R_{0023;2}$ (same as J^3) and $R_{0123;2}$, (centered on the 1-3 face at half time steps).

This differencing scheme has a number of properties that make it look like a finite implementation of differential calculus. First, the differential operator, which creates a tensor of one higher order (*e.g.*, equation 11), naturally places the new tensor on the proper grid if the differencing is centered. This is also true of the generation of $\Gamma_{\alpha\beta\gamma}$ from the metric field $g_{\alpha\beta}$. Second, one of the most fundamental properties of a spacetime, the covariant derivative of the metric ($g_{\alpha\beta;\gamma}$) vanishes, is naturally satisfied to machine accuracy because of this property. Third, the contraction of a mixed tensor is trivial: for each staggered component of the contracted tensor the four components of the parent tensor that are needed for the sum are already located at the same grid point as the contracted component. No additional averaging is needed. Fourth, as shown below, in a local Riemann normal coordinate system, the Bianchi identities are satisfied to machine accuracy. All terms cancel exactly, so the constraints are propagated exactly as well.

Certain special tensors also have interesting properties. The Kronecker delta δ^α_β , for example, has non-zero elements (unity) only at hypercube cell corners. This is also true of other identity tensors ($\delta^{\alpha\beta}_{\lambda\mu}$, $\delta^{\alpha\beta\gamma}_{\lambda\mu\nu}$, *etc.*), which are ± 1 at cell corners. The Levi-Civita tensor $\epsilon_{\alpha\beta\gamma\delta}$ and anti-symmetric symbol $[\alpha\beta\gamma\delta]$ are just the opposite. They are zero everywhere except at the hypercube *body centers*. They look much like the identity tensors, but on a grid that is shifted one-half step in each dimension. Furthermore, as the Levi-Civita tensor expresses the volume element

$$\epsilon_{\alpha\beta\gamma\delta} = \sqrt{-g} [\alpha\beta\gamma\delta]$$

its placement at the hypercube center creates a natural scheme for forming volume integrals over those hypercubes.

5. CT for Numerical Relativity

5.1. Statement of the Problem

For reasons that are developed more fully below, we will use mixed tensors to define the problem of numerical relativity. As noted above, such tensors will lend themselves easily to contraction.

The classic problem of general relativity is to solve Einstein's field equations

$$G^\alpha_\beta = 8\pi T^\alpha_\beta \tag{20}$$

($c = G = 1$) for the metric coefficients. The Einstein curvature tensor is derived from the Ricci curvature tensor

$$G^\alpha_\beta \equiv R^\alpha_\beta - \frac{1}{2}\delta^\alpha_\beta R \tag{21}$$

with

$$R \equiv R^\alpha_\alpha \quad (22)$$

being the Ricci curvature scalar. The Ricci tensor is the contraction of the Riemann tensor on the first and third indices

$$R^\alpha_\beta \equiv R^{\mu\alpha}_{\mu\beta} \quad (23)$$

The Riemann tensor is the full statement of curvature of the spacetime. In its mixed form it is given by

$$R^{\alpha\beta}_{\gamma\delta} = \Gamma^{\alpha\beta}_{\delta,\gamma} - \Gamma^{\alpha\beta}_{\gamma,\delta} + \Gamma^{\alpha\mu}_{\delta}\Gamma^{\beta}_{\mu\gamma} - \Gamma^{\alpha\mu}_{\gamma}\Gamma^{\beta}_{\mu\delta} \quad (24)$$

for a coordinate basis. The doubly-raised connection coefficients are given by

$$\Gamma^{\alpha\beta}_{\gamma} \equiv g^{\beta\nu}\Gamma^{\alpha}_{\nu\gamma} \quad (25)$$

We assume that the metric $g_{\alpha\beta}$ has a unique inverse $g^{\alpha\beta}$ such that

$$g^{\alpha\mu}g_{\mu\beta} = \delta^\alpha_\beta \quad (26)$$

In this paper we will treat only the vacuum problem (the source of stress-energy $T^\alpha_\beta = 0$) so that equation (20) becomes

$$R^\alpha_\beta = G^\alpha_\beta = 0 \quad (27)$$

The Riemann tensor $R^{\alpha\beta}_{\gamma\delta}$ possesses several symmetries, including algebraic antisymmetry on α and β (and on γ and δ) and differential symmetries (Bianchi identities)

$$R^{\alpha\beta}_{[\gamma\delta;\epsilon]} \equiv R^{\alpha\beta}_{\gamma\delta;\epsilon} + R^{\alpha\beta}_{\epsilon\gamma;\delta} + R^{\alpha\beta}_{\delta\epsilon;\gamma} = 0 \quad (28)$$

The reader will note that the mixed Riemann tensor is missing one additional symmetry that is possessed by the covariant version: $R_{\alpha\beta\gamma\delta} = R_{\gamma\delta\alpha\beta}$. (A raised index cannot be swapped with a lower one.) When contracted on the first and third indices, the Bianchi identities become simply

$$R^\alpha_{\beta;\alpha} - \frac{1}{2}R_{,\beta} = G^\alpha_{\beta;\alpha} = 0 \quad (29)$$

i.e., the divergence free condition on the Einstein tensor. These four conditions are responsible for propagating the four constraints

$$G^0_\beta = 0 \quad (30)$$

if the other equations are satisfied

$$G^i_\beta = 0 \quad (31)$$

5.2. CT in Riemann Normal Coordinates

At any point P in spacetime one can construct many transformations $L^{\alpha}_{\hat{\beta}}$ to locally Lorentz systems such that

$$g_{\hat{\alpha}\hat{\beta}} = L^{\mu}_{\hat{\alpha}} L^{\nu}_{\hat{\beta}} g_{\mu\nu} = \eta_{\hat{\alpha}\hat{\beta}} \quad (32)$$

in a neighborhood of that point. However, only one of those systems — the Riemann normal system — also has vanishing *gradients* of the metric and, therefore, vanishing connection coefficients in that same neighborhood

$$\begin{aligned} g_{\hat{\alpha}\hat{\beta},\hat{\gamma}} &= 0 \\ \Gamma_{\hat{\alpha}\hat{\beta}\hat{\gamma}} &= 0 \end{aligned}$$

In this coordinate system, in the neighborhood of P , covariant derivatives become ordinary derivatives and the Riemann tensor and its Bianchi identities become

$$R^{\hat{\alpha}\hat{\beta}}_{\hat{\gamma}\hat{\delta}} = \Gamma^{\hat{\alpha}\hat{\beta}}_{\hat{\delta},\hat{\gamma}} - \Gamma^{\hat{\alpha}\hat{\beta}}_{\hat{\gamma},\hat{\delta}} \quad (33)$$

$$R^{\hat{\alpha}\hat{\beta}}_{[\hat{\gamma}\hat{\delta};\hat{\epsilon}]} = \Gamma^{\hat{\alpha}\hat{\beta}}_{\hat{\delta},\hat{\gamma}\hat{\epsilon}} - \Gamma^{\hat{\alpha}\hat{\beta}}_{\hat{\gamma},\hat{\delta}\hat{\epsilon}} + \Gamma^{\hat{\alpha}\hat{\beta}}_{\hat{\gamma},\hat{\epsilon}\hat{\delta}} - \Gamma^{\hat{\alpha}\hat{\beta}}_{\hat{\epsilon},\hat{\gamma}\hat{\delta}} + \Gamma^{\hat{\alpha}\hat{\beta}}_{\hat{\epsilon},\hat{\delta}\hat{\gamma}} - \Gamma^{\hat{\alpha}\hat{\beta}}_{\hat{\delta},\hat{\epsilon}\hat{\gamma}} = 0 \quad (34)$$

In the proposed staggered grid scheme in the previous section, each of the terms of $R^{\hat{\alpha}\hat{\beta}}_{[\hat{\gamma}\hat{\delta};\hat{\epsilon}]}$ would be evaluated at the same grid point, because they each have the same five indices. So the sum can be accomplished without additional averaging from other grid points. We further note that each term has a duplicate with the opposite sign, differing only in the order of the derivatives (*e.g.*, $\Gamma^{\hat{\alpha}\hat{\beta}}_{\hat{\delta},\hat{\gamma}\hat{\epsilon}} - \Gamma^{\hat{\alpha}\hat{\beta}}_{\hat{\delta},\hat{\epsilon}\hat{\gamma}}$). We can therefore draw the following conclusion: *If a numerical scheme is constructed such that derivatives commute (both space-space and space-time), then in Riemann normal coordinates the equation for the Bianchi identities (34) will be satisfied to machine accuracy, resulting in the propagation of the constraints to machine accuracy.* We note that the scheme proposed in Section 4 possesses the required properties.

How does satisfying the Bianchi identities propagate the constraints numerically? This is easy to show in Riemann normal coordinates. For the vacuum problem, the constraints are given by

$$R^{\hat{0}}_{\hat{\beta}} = 0 \quad (35)$$

and we seek a scheme in which the constraints propagate to machine accuracy

$$R^{\hat{0}}_{\hat{\beta},\hat{0}} = O(\epsilon_r) \quad (36)$$

But satisfying the Bianchi identities (equation 34) will mean that the contracted identities are also satisfied to machine accuracy

$$R^{\hat{\alpha}}_{\hat{\beta},\hat{\alpha}} = O(\epsilon_r) \quad (37)$$

or

$$\mathbf{R}^{\hat{\beta}, \hat{0}} = -\mathbf{R}^{\hat{i}, \hat{\beta}, \hat{i}} + O(\epsilon_r) \quad (38)$$

All that needs to be shown is that $\mathbf{R}^{\hat{i}, \hat{\beta}, \hat{i}} = O(\epsilon_r)$ also. For the three momentum constraints ($\hat{\beta} = \hat{j}$) this is straightforward, because $\mathbf{R}^{\hat{i}, \hat{j}} = 0$ are the field equations being computed, so $\mathbf{R}^{\hat{i}, \hat{j}}$ is $O(\epsilon_r)$ by definition.² So the spatial gradients $\mathbf{R}^{\hat{i}, \hat{j}, \hat{i}}$ will be $O(\epsilon_r)$, thereby propagating $\mathbf{R}^{\hat{0}, \hat{j}}$ to machine accuracy.

For the Hamiltonian constraint ($\hat{\beta} = 0$) we require satisfaction of the momentum constraints on the hypersurface, *i.e.*, $\mathbf{R}^{\hat{i}, \hat{0}, \hat{i}} = O(\epsilon_r)$. Therefore, as long as the momentum constraints propagate to machine accuracy on each hypersurface, which we have shown above to be the case, the Hamiltonian constraint will propagate also. Note, however, if the gradient of the momentum constraints has a constant bias, then the Hamiltonian constraint will grow. On the other hand, if the divergence fluctuates randomly, the the Hamiltonian constraint will fluctuate only randomly as well.

5.3. CT in a General Coordinate Basis

Because a Riemann normal coordinate system is local only and cannot be used to cover the entire spacetime, we are forced to deal with non-zero connection coefficients. But we still will attempt to propagate the constraints in the same manner — with a scheme that enforces the Bianchi identities by employing temporal and spatial differences that commute.

5.3.1. Propagation of the Constraints

It is important to note that the Bianchi identities are never *explicitly* calculated in the CT method. Instead, we develop a scheme in which

$$\mathbf{R}^0_{\beta, 0} = 0$$

²This statement requires a little clarification. Of course, the *solution* of $\mathbf{R}^{\hat{i}, \hat{j}} = 0$ is accurate to only $O(\epsilon_{tr})$. However, if we use this truncation-accurate solution to re-compute $\mathbf{R}^{\hat{i}, \hat{j}}$, *using exactly the same mathematical definition of terms that we used in the evolution equation*, then that re-computed $\mathbf{R}^{\hat{i}, \hat{j}}$ will be zero to machine accuracy. (It will not be so only if we use a different differencing scheme than the one used in the original evolution equation.) As a simple example, consider a line of code that computes $y = ax + b$. Then, if we later compute the function $f = y - ax - b$, by definition, f will be zero to machine accuracy.

is satisfied to at least truncation accuracy for all time. (We will find that machine accuracy may be an unattainable goal.) However, in a general coordinate system, the update of R^0_β will depend on an “advection” of curvature from surrounding cells, due to the covariant derivative connection terms. So, we equivalently seek a scheme in which

$$R^0_{\beta;0} = 0 \quad (39)$$

to at least truncation accuracy. If we set up a grid in which

$$R^{\alpha\beta}_{[\gamma\delta;\epsilon]} = O(\epsilon_{tr}) \quad (40)$$

then we can proceed in much the same manner as in Riemann normal coordinates, but with covariant derivatives. If the Bianchi identities are satisfied to truncation accuracy, then their contracted form also will hold

$$\begin{aligned} R^0_{0;0} &= -R^j_{0;j} + O(\epsilon_{tr}) \\ R^0_{i;0} &= -R^j_{i;j} + O(\epsilon_{tr}) \end{aligned}$$

So, if the momentum constraints are satisfied on each hypersurface, the Hamiltonian constraint will propagate, albeit along geodesics, not coordinate lines. And the momentum constraints will propagate if the field equations are satisfied to at least truncation accuracy.

5.3.2. Cancellation of the $\partial^2\Gamma$ Terms

In order to demonstrate cancellation of terms in the Bianchi identities, we choose the following form for the mixed Riemann tensor

$$\begin{aligned} R^{\alpha\beta}_{\gamma\delta} &= \frac{1}{2} \left(\Gamma^{\alpha\beta}_{\delta,\gamma} - \Gamma^{\alpha\beta}_{\gamma,\delta} - \Gamma^{\beta\alpha}_{\delta,\gamma} + \Gamma^{\beta\alpha}_{\gamma,\delta} \right. \\ &\quad \left. + \Gamma^{\alpha\mu}_{\delta} \Gamma^{\beta}_{\mu\gamma} - \Gamma^{\alpha\mu}_{\gamma} \Gamma^{\beta}_{\mu\delta} + \Gamma^{\alpha}_{\mu\delta} \Gamma^{\beta\mu}_{\gamma} - \Gamma^{\alpha}_{\mu\gamma} \Gamma^{\beta\mu}_{\delta} \right) \end{aligned} \quad (41)$$

with the singly-raised connection coefficient *re*-computed from the doubly-raised ones and the gradient of the inverse metric

$$\Gamma^{\beta}_{\mu\gamma} = \frac{g^{\mu\nu}}{2} \left(\Gamma^{\beta\nu}_{\gamma} - \Gamma^{\nu\beta}_{\gamma} - g^{\beta\nu}_{,\gamma} \right) \quad (42)$$

This form has the following properties

1. $R^{\alpha\beta}_{\gamma\delta}$ possesses explicitly all of the algebraic symmetries discussed in Section 5.1.

2. When the Bianchi identities are formed³

$$\begin{aligned}
 & \mathbf{R}^{\alpha\beta}_{\gamma\delta,\varepsilon} + \Gamma^{\alpha}_{\mu\varepsilon} \mathbf{R}^{\mu\beta}_{\gamma\delta} + \Gamma^{\beta}_{\mu\varepsilon} \mathbf{R}^{\alpha\mu}_{\gamma\delta} + \\
 & \mathbf{R}^{\alpha\beta}_{\varepsilon\gamma,\delta} + \Gamma^{\alpha}_{\mu\delta} \mathbf{R}^{\mu\beta}_{\varepsilon\gamma} + \Gamma^{\beta}_{\mu\delta} \mathbf{R}^{\alpha\mu}_{\varepsilon\gamma} + \\
 & \mathbf{R}^{\alpha\beta}_{\delta\varepsilon,\gamma} + \Gamma^{\alpha}_{\mu\gamma} \mathbf{R}^{\mu\beta}_{\delta\varepsilon} + \Gamma^{\beta}_{\mu\gamma} \mathbf{R}^{\alpha\mu}_{\delta\varepsilon} = 0
 \end{aligned} \tag{43}$$

and equation (42) is inserted, the $\Gamma^{\alpha\beta}_{\gamma,\delta\varepsilon}$ terms will cancel *to machine accuracy*, as described before in section 5.2.

5.3.3. Cancellation of the $\Gamma\partial\Gamma$ Terms

In equation (43) the $\Gamma^{\alpha}_{\mu\varepsilon} \Gamma^{\mu\beta}_{\delta,\gamma}$ terms will cancel explicitly *algebraically*. Will they cancel numerically also? The answer is yes, if we apply the following numerical procedures

1. Use linear interpolation (averaging) to determine quantities at intermediate grid points
2. When forming a product, such as $g_{\mu\nu} \Gamma^{\beta\nu}_{\gamma}$, first average the factors to the grid point in question, then form the products and finally the sum. Do not form the products on different grid points and then average.

Consider, for example, the two following Bianchi identity terms

$$\Gamma^{\alpha\mu}_{\delta,\varepsilon} \Gamma^{\beta}_{\mu\gamma} - \Gamma^{\beta}_{\mu\gamma} \Gamma^{\alpha\mu}_{\delta,\varepsilon} \tag{44}$$

Algebraically, of course, the two terms cancel. However, in a staggered grid scheme they are not computed in the same manner. The first term comes from *differencing* a $\Gamma\Gamma$ term in the first term of equation (43), while the second comes from the *connection* of one of the $\partial\Gamma$ terms in the last term of that same equation. One is the difference of an average, while the other is the average of differences. But, with linear averaging, we see that, under these conditions, the chain rule is satisfied to machine accuracy

$$\begin{aligned}
 {}_0 \left[\Gamma^{\alpha\mu}_{\delta} \Gamma^{\beta}_{\mu\gamma} \right]_{,\varepsilon} &= \frac{1}{\Delta x^{\varepsilon}} \left\{ \frac{1}{2} \left[\Gamma^{\alpha\mu}_{\delta} \Gamma^{\beta}_{\mu\gamma} \right] - \frac{1}{2} \left[\Gamma^{\alpha\mu}_{\delta} \Gamma^{\beta}_{\mu\gamma} \right] \right\} \\
 &= \frac{1}{\Delta x^{\varepsilon}} \left\{ \left[\frac{1}{2} \Gamma^{\alpha\mu}_{\delta} - \frac{1}{2} \Gamma^{\alpha\mu}_{\delta} \right] \left[\frac{1}{2} \left(\frac{1}{2} \Gamma^{\beta}_{\mu\gamma} + \frac{1}{2} \Gamma^{\beta}_{\mu\gamma} \right) \right] \right\}
 \end{aligned}$$

³Note that, because of the antisymmetry in the last two indices of $\mathbf{R}^{\alpha\beta}_{\gamma\delta}$ and the symmetry in the last two indices of $\Gamma^{\alpha}_{\beta\gamma}$, the connection terms involving γ and δ will cancel, just as they did for the antisymmetric Faraday tensor Bianchi identities in equation (18).

$$\begin{aligned}
& + \left[\frac{1}{2} \left(\frac{1}{2} \Gamma^{\alpha\mu}_{\delta} + -\frac{1}{2} \Gamma^{\alpha\mu}_{\delta} \right) \right] \left[\frac{1}{2} \Gamma^{\beta}_{\mu\gamma} - -\frac{1}{2} \Gamma^{\beta}_{\mu\gamma} \right] \Big\} \\
& = {}_0 \left(\Gamma^{\alpha\mu}_{\delta,\varepsilon} \Gamma^{\beta}_{\mu\gamma} \right) + {}_0 \left(\Gamma^{\alpha\mu}_{\delta} \Gamma^{\beta}_{\mu\gamma,\varepsilon} \right) \tag{45}
\end{aligned}$$

where the pre-appended subscript $\frac{1}{2}$ signifies the spatial node position at which that quantity is evaluated, *e.g.*, $\frac{1}{2}x^{\varepsilon} = \frac{1}{2}({}_1x^{\varepsilon} + {}_0x^{\varepsilon})$, and the quantities $\frac{1}{2}\Gamma^{\alpha\mu}_{\delta}$ are themselves averages

$$\frac{1}{2}\Gamma^{\alpha\mu}_{\delta} = \frac{1}{2}({}_1\Gamma^{\alpha\mu}_{\delta} + {}_0\Gamma^{\alpha\mu}_{\delta}) \tag{46}$$

So, the differencing of a $\Gamma\Gamma$ term will produce two averaged $\Gamma\partial\Gamma$ terms. In addition, averaging factors *before* forming products causes the average and difference operators to commute, so that the second term in (44) becomes

$$\begin{aligned}
-{}_0 \left(\Gamma^{\beta}_{\mu\gamma} \Gamma^{\alpha\mu}_{\delta,\varepsilon} \right) & = -\frac{1}{2} \left[\frac{1}{2} \Gamma^{\beta}_{\mu\gamma} + -\frac{1}{2} \Gamma^{\beta}_{\mu\gamma} \right] \frac{1}{2} \left[\frac{1}{2} \Gamma^{\alpha\mu}_{\delta,\varepsilon} + -\frac{1}{2} \Gamma^{\alpha\mu}_{\delta,\varepsilon} \right] \\
& = -\frac{1}{2} \left[\frac{1}{2} \Gamma^{\beta}_{\mu\gamma} + -\frac{1}{2} \Gamma^{\beta}_{\mu\gamma} \right] \frac{1}{2\Delta x^{\varepsilon}} \left[({}_1\Gamma^{\alpha\mu}_{\delta} - {}_0\Gamma^{\alpha\mu}_{\delta}) + ({}_0\Gamma^{\alpha\mu}_{\delta} - {}_{-1}\Gamma^{\alpha\mu}_{\delta}) \right] \\
& = -\frac{1}{2} \left[\frac{1}{2} \Gamma^{\beta}_{\mu\gamma} + -\frac{1}{2} \Gamma^{\beta}_{\mu\gamma} \right] \frac{1}{\Delta x^{\varepsilon}} \left[\frac{1}{2}({}_1\Gamma^{\alpha\mu}_{\delta} + {}_0\Gamma^{\alpha\mu}_{\delta}) - \frac{1}{2}({}_0\Gamma^{\alpha\mu}_{\delta} + {}_{-1}\Gamma^{\alpha\mu}_{\delta}) \right] \\
& = -\frac{1}{2} \left[\frac{1}{2} \Gamma^{\beta}_{\mu\gamma} + -\frac{1}{2} \Gamma^{\beta}_{\mu\gamma} \right] \frac{1}{\Delta x^{\varepsilon}} \left[\frac{1}{2} \Gamma^{\alpha\mu}_{\delta} - -\frac{1}{2} \Gamma^{\alpha\mu}_{\delta} \right] \\
& = -{}_0 \Gamma^{\beta}_{\mu\gamma} {}_0 \Gamma^{\alpha\mu}_{\delta,\varepsilon}
\end{aligned}$$

which exactly cancels the first term on the right side of equation (45). A similar process with another $-\Gamma\partial\Gamma$ term will cancel the second term on the right side of that equation.

5.3.4. Non-cancellation of the Γ^3 Terms

While we are reasonably confident that, with these measures, $\Gamma\partial\Gamma$ terms in the Bianchi identities will cancel, it is clear that the Γ^3 terms will *not* cancel to machine accuracy. These are all produced by connection of the double- Γ terms in the Riemann tensor. However, when forming the Bianchi identities, the connection takes place on an already-multiplied and summed $\Gamma\Gamma$ product. One cannot undo the sums and products, form averages, and then re-form the triple- Γ product. And the product of averages does *not* commute with the average of products. The Bianchi identities, therefore, will be left with terms proportional to the truncation error and $(\partial g)^3$. Unless some clever averaging scheme can be found to allow the triple- Γ terms to also cancel to machine accuracy, any CT scheme developed along these lines will be subject to truncation error. The hope, then, is that cancellation of second and first order derivatives of the connection (third and second order derivatives of the metric coefficients) will be sufficient to improve the stability of the discrete evolution scheme.

Therefore, while the staggered grid CT method clearly works in Riemann normal coordinates, detailed numerical experiments will be needed to see if it maintains its desirable properties when applied in a general coordinate basis.

5.4. Numerical Implementation

5.4.1. General Iterative Approach

The goal of this CT scheme is to produce an interlocking, staggered four-dimensional grid of $g_{\alpha\beta}$ tensor values by successively adding new half and whole temporal hypersurfaces. Because interpolation is in time, as well as space, the scheme necessarily will be an implicit one and, therefore, iterative. Our approach then will be to first produce an initial guess for $g_{\alpha\beta}$ on the next level of hypersurfaces using an existing explicit scheme. This solution will not satisfy the interlocking staggered grid equations, so it will be iterated using the latter until it does. The exact iterative scheme is still under development, but one possible implementation is a multigrid technique in which the variables are the spatial g_{ij} and the equations are the $R^i_j = 0$ field equations.

This method appears similar to recently-suggested approaches in which the constraints are re-solved at each time step. There are, however, two key differences. First, the constraints are not solved explicitly. Instead, the evolution equations are solved in such a way that they are implicitly enforced. This ensures a scheme in which the evolution and constraints are fully compatible and not tracking different numerical solutions to the differential equations. Secondly, the equations being iterated are implicit hyperbolic, not elliptic. In addition to information on the new hypersurface, at each iteration these equations utilize information from the *previous* hypersurface — information that constraint equations do not have. With this added information, if implemented properly, the iterative scheme should exhibit faster convergence than a regular constraint solver would have.

Figure 5 shows implementation of a simple 1+1 space-time problem. Comparison of this figure with Figure 4 will give insight into implementation of the full 4-D interlocking grid. ${}^n g_{00}$ and ${}^n g_{11}$ are quantities known from the previous time step, the first being a gauge condition and the second being the solution. ${}^{n+\frac{1}{2}} g_{10}$ and ${}^{n+1} g_{00}$ are gauge conditions on the *new* hypersurfaces, and ${}^{n+1} g_{11}$ is the new solution that will be determined by the iterative numerical scheme.

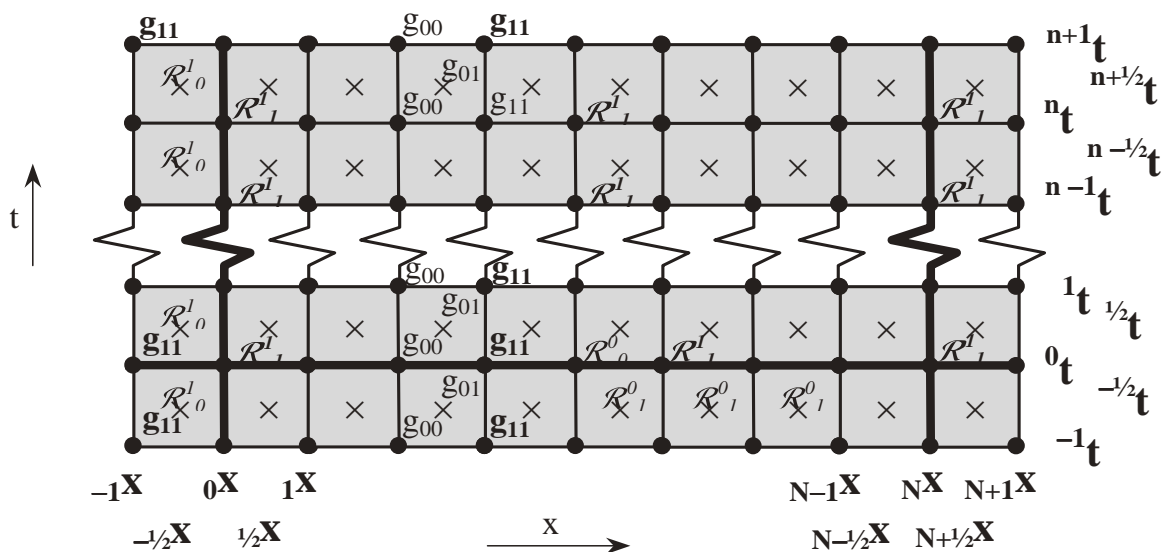


Fig. 5.— Illustration of a 1+1 field evolution, including the initial data problem at 0t and a one-point boundary data problem at 0x . Bold quantities on the grid are solutions to the initial data and evolutionary problems. The computation begins by using gauge conditions to specify g_{00} at ${}^{-1}t$, 0t , and 1t and g_{01} at ${}^{-\frac{1}{2}t}$ and ${}^{\frac{1}{2}t}$. Then R^0_1 , R^0_0 , and R^1_1 are solved for g_{11} at ${}^{-1}t$, 0t , and 1t . At the 0x boundary g_{11} may be specified, but at the ${}^{-1}x$ boundary g_{11} must be consistent with $R^1_0 = 0$. Similarly, the g_{11} at ${}_{N+1}x$ are obtained by solving $R^1_0 = 0$ at ${}_{N+\frac{1}{2}}x$. The evolution from nt to ${}^{n+1}t$ proceeds by specifying g_{01} at ${}^{n+\frac{1}{2}}t$ and g_{00} at ${}^{n+1}t$. g_{11} is computed by solving $R^1_1 = 0$. The boundary conditions $R^1_0 = 0$ also must be applied at $({}^{n+\frac{1}{2}}t, {}^{-\frac{1}{2}}x)$ and $({}^{n+\frac{1}{2}}t, {}_{N+\frac{1}{2}}x)$ to obtain g_{11} at ${}^{-1}x$ and ${}_{N+1}x$ on the new hypersurface.

5.4.2. Using Gauge Conditions and Time Stepping

Specification of the coordinate gauge is similar to doing so in classic 3+1 schemes: g_{00} is freely specified at cube corners on whole hypersurfaces, and g_{0i} is freely specified at cube edge centers on half hypersurfaces. g_{0i} is related to the shift vector $\beta^i = g^{0i}$, and both are properly located at half time steps vector points. $g_{00} = -\alpha^2 + g_{ij}\beta^i\beta^j$ is related to the lapse α , and properly located in this scheme at scalar points. The g_{ij} are the six unique gravitational potential fields that we intend to solve.

A typical time step then begins with $g_{\alpha\beta}$ components known on hypersurfaces ^{n-1}t , $^{n-\frac{1}{2}}t$, and nt . One then specifies the g_{0i} vector on hypersurface $^{n+\frac{1}{2}}t$ and the g_{00} scalar at ^{n+1}t . The explicit predictors for g_{ij} at ^{n+1}t then complete the new $g_{\alpha\beta}$ field, and the iteration on the g_{ij} can then begin. If the $g_{0\alpha}$ are dependent on the g_{ij} field (which generally will be the case here), then the gauge conditions need to be updated at each iteration for a consistent solution.

5.4.3. Constructing the Inverse Metric

The inverse of $g_{\alpha\beta}$ is often needed to raise the connection coefficients for use in the evolution equations. In principle these $g^{\alpha\beta}$ should also be located at second-ranked tensor grid points. In practice, however, we never need the actual staggered $g^{\alpha\beta}$ fields. Instead, we need their interpolated averages $\bar{g}^{\alpha\beta}$ at third-ranked tensor points. Furthermore, in order for the raising and lowering of connection coefficient indices to commute, the staggered field of $g^{\alpha\beta}$ values must be constructed in such a way that its average, and that of $g_{\alpha\beta}$, are orthogonal at those third-ranked tensor points

$$\bar{g}^{\alpha\mu} \bar{g}_{\mu\beta} = \delta^{\alpha}_{\beta} \quad (47)$$

So construction of the index-raising tensor $\bar{g}^{\alpha\beta}$ is a straightforward matter of averaging $g_{\alpha\beta}$ to places where the $\Gamma_{\alpha\beta\gamma}$ are computed, and then inverting that average *locally* at those grid points. The actual staggered fields of $g^{\alpha\beta}$ values, whose averages should give us these $\bar{g}^{\alpha\beta}$ at third-ranked tensor points, never need to be determined. This procedure is fast, gives us raising and lowering operators that commute, and follows the afore-mentioned rule of averaging first and then multiplying and summing second.

5.4.4. The Initial Data Problem

The initial data problem for a staggered grid will be a little more complicated than that for a non-staggered scheme. In the latter case, there are 12 unknowns (g_{ij} and $g_{ij,0}$) and four equations

($R^0_\beta = 0$) on the initial hypersurface at $t = {}^0t$, for a net total of eight degrees of freedom. In the staggered case, R^0_0 is computed at $t = {}^0t$, but the R^0_j are computed at $t = -\frac{1}{2}t$.

Solution of the momentum constraints, given g_{ij} at $t = {}^0t$, is fairly straightforward in the staggered case. They are not functions of second-order time derivatives of the metric (e.g., $g_{ij,00}$), so the placement of those constraints at $t = -\frac{1}{2}t$ allows them to directly relate ${}^{-1}g_{ij}$ at to ${}^0g_{ij}$. All Γ s can be computed in a staggered manner. The momentum constraint solution at $-\frac{1}{2}t$, then, would have six unknowns (${}^0g_{ij}$) and three constraints, leaving three degrees of freedom, just like the non-staggered grid case.

The Hamiltonian constraint, however, presents a problem. While R^0_0 also does not involve any second-order time derivatives, nevertheless it does involve *first* order time derivatives $g_{ij,0}$. Those still are defined on half-hypersurfaces and, therefore, need to be *interpolated* to 0t . That is, we need the $g_{ij,0}$ at both $-\frac{1}{2}t$ and $\frac{1}{2}t$ anyway, even if we are not going to compute $g_{ij,00}$. At first glance there does not appear to be a method of providing an accurate $g_{ij,0}(t)$ field to properly compute this interpolation. Of course, one simply could extrapolate $g_{ij,0}$ at $-\frac{1}{2}t$ forward to 0t (i.e., assume $g_{ij,00} = 0$) and then solve $R^0_0 = 0$ there. The Hamiltonian constraint solution then would have the six g_{ij} unknowns and one constraint — five degrees of freedom — just like the non-staggered case.

But a serious problem still remains. *There is no means of enforcing the Hamiltonian constraint at $t = {}^1t$.* While the staggered grid is, in principle, capable of doing that, it can do so only through the evolution equations $R^i_j = 0$. But at this stage we have not yet begun to enforce the evolution. One possible method of solving this is to do nothing. Just accept the fact that, at $t = {}^1t$, $R^0_0 = 0$ is good only to truncation accuracy. Choosing a very small Δt (a “thin sandwich”) would keep this error small. A second approach would be to also explicitly enforce the constraint on $t = {}^1t$, which would reduce the number of degrees of freedom of the Hamiltonian problem from five to four. While producing a more constrained problem, this solution would result in two successive hypersurfaces on which the Hamiltonian constraint is satisfied. Yet a third alternative would be to locate R^0_j on the $\frac{1}{2}t$ hypersurface and extrapolate quantities like $g_{ij,0}$ *forward* to 1t . The problem with this approach is that, while the Hamiltonian constraint is satisfied for the *extrapolated* $g_{ij,0}$ field, when the evolution is begun, the Hamiltonian constraint that is implicit in the evolution equations will use fields that are *interpolated* in time between $-\frac{1}{2}t$ and $\frac{1}{2}t$. There will be, therefore, an implicit constraint violation injected into the evolution at the outset.

The elegant, and proper, method of solving this problem is to *solve all ten of the Einstein field equations simultaneously on the initial hypersurfaces*. There will be 18 unknowns (g_{ij} at ${}^{-1}t$, 0t , and 1t) and 10 equations, leaving 8 degrees of freedom, just like the non-staggered case. The resulting fields will be properly staggered, and the Γ s will be properly staggered and interpolated.

The Hamiltonian constraint will be satisfied at 0t using the correctly interpolated fields, and it will be satisfied at 1t (and even ${}^{-1}t$) as well, because the evolution equations (and therefore the Bianchi identities) are fully enforced. Similarly, the momentum constraints will be satisfied at ${}^{-\frac{1}{2}}t$ and ${}^{\frac{1}{2}}t$ for the same reason, regardless of whether they are actually applied at ${}^{-\frac{1}{2}}t$ or at ${}^{\frac{1}{2}}t$. The reader will, of course, recognize that this is more than solving an initial data problem; in actuality the proposed scheme solves the initial data problem plus the first full evolutionary time step simultaneously. This is done to ensure that the initial data on the first three hypersurfaces are solutions of the discrete, staggered evolutionary field equations. No constraint violation will be introduced implicitly other than what is naturally present in the evolutionary method already.

5.4.5. Boundary Conditions

One-point Boundary Conditions

When \mathbf{g} and $\mathbf{n} \cdot \nabla \mathbf{g}$ are specified on the same boundary, where \mathbf{n} is the boundary normal, the boundary data problem is similar to the initial data problem. In all such cases, the boundary constraints are given by

$$n_\mu R^\mu{}_\beta = 0 \quad (48)$$

and for rectilinear grids with the boundary normal being a coordinate unit 1-form $\mathbf{n} = \mathbf{w}^{(i)}$, this yields

$$R^{(i)}{}_\beta = 0 \quad (49)$$

where the symbol (i) is a label indicating the boundary direction in question, not strictly a coordinate index. The equation $R^{(i)}{}_i$ (no sum) is located at 3-cube corners and plays the role of boundary constraint in much the same manner as the Hamiltonian constraint does at 0t . Similarly, the equations $R^{(i)}{}_a = 0$ ($a \neq i$) play the same role as the momentum constraints did earlier. By analogy, then, the boundary problem is as follows. There are 12 unknowns (g_{ab} [$a \neq i, b \neq i$] at $x^{(i)} = {}_0x^{(i)}$ and at $x^{(i)} = {}_{-1}x^{(i)}$, *i.e.*, on the i^{th} boundary and one ghost node *beyond* the boundary), and there are 4 equations (49). This leaves 8 degrees of freedom again, which must be specified with additional boundary conditions. The diagonal constraint $R^{(i)}{}_i = 0$ is applied at ${}_0x^{(i)}$ at 3-cube corners.

Two of the off-diagonal constraints ($R^{(i)}{}_j = 0$ [$j \neq i$]) are applied on whole hypersurfaces at ${}_{-\frac{1}{2}}x^{(i)}$, and the final constraint $R^{(i)}{}_0 = 0$ is applied also at ${}_{-\frac{1}{2}}x^{(i)}$ but on time half-hypersurfaces. The reader will note that this latter set of equations is related to the set of momentum constraints $R^{(0)}{}_i = 0$, but the momentum constraints are defined at ${}^{\frac{1}{2}}x^{(i)}, {}^{\frac{3}{2}}x^{(i)}, {}^{\frac{5}{2}}x^{(i)}, \dots, {}^{N+\frac{1}{2}}x^{(i)}$ and propagated

forward by the evolution equations. The constraint at $_{-1/2}x^{(i)}$ must be explicitly enforced in most cases, along with the three others and the eight freely-specified $g_{\alpha\beta}$ at $_{-1}x^{(i)}$ and $_{0}x^{(i)}$.

Two-point Boundary Conditions

Any number of additional boundary data problems are possible. $R^{(i)}_a = 0$ could be specified at the upper (i) boundary, while $R^{(i)}_i = 0$ could be specified at the lower (i) boundary, for example. Also, some of the eight free $g_{\alpha\beta}$ could be specified on opposing boundaries as well.

For periodic boundary conditions, the six unknown $g_{\alpha\beta}$ at $_{-1}x^{(i)}$ are set to those near $_{N}x^{(i)}$, and those at $_{N+1}x^{(i)}$ are set to those near $_{0}x^{(i)}$. No constraints are applied explicitly, only implicitly through the wrapping conditions and the evolutionary solution of the field equations.

5.4.6. Implementation Summary

It is useful to summarize how a complete problem will proceed. The computation begins by using gauge conditions to specify g_{00} at ^{-1}t , 0t , and 1t and g_{0i} at $^{-1/2}t$ and $^{1/2}t$. The full initial data plus time-step problem, including the field equations, is then solved for g_{ij} on ^{-1}t , 0t , and 1t , applying eight freely-specified g_{ij} (or eight functions thereof) in the process. Appropriate boundary constraints also need to be applied in order to obtain a consistent solution.

The field equations are generated as follows. An initial guess for the g_{ij} is obtained by some means, perhaps using conformal or other existing initial value methods or, for the evolution, an explicit forward integration scheme. The full $g_{\alpha\beta}$ field values then are differenced onto third-rank tensor grid points, and the $\Gamma_{\alpha\beta\gamma}$ are formed. The $g_{\alpha\beta}$ values are also averaged to those same third-rank tensor points, and an inverse of that average $\bar{g}^{\alpha\beta}$ is used to raise the connection coefficients (equations 16 and 25). The Γ s, in turn, then are differenced and averaged to second-rank tensor points for the Riemann tensor calculation. (Note that there will be no need for values at other fourth-rank tensor points [hypercube body centers], as Riemann will be immediately contracted into Ricci.) Equation (24) should suffice for the Riemann calculation (*i.e.*, the explicit version [equation 41] should not be needed), because our raising and lowering operators commute, rendering the results of equations (16) and (42) the same to machine accuracy. Contraction to Ricci is trivial, as it sums Riemann components already computed at second-rank tensor points, and the R^i_j are then tested to see if they are zero. If not, the local values of g_{ij} are modified in an appropriate manner, and the computation of the Ricci components is repeated until convergence. It is important to remember that at grid boundaries, the boundary constraints (which are evolutionary equations in their own right) must be applied and iterated upon as well, and the freely-specified boundary conditions must be applied.

When the iterative solution is acceptable, the computation continues to the next hypersurface, first specifying the gauge conditions and then solving the field equations.

6. Discussion

The largest uncertainty in the proposed method is the effect of the truncation errors introduced by non-cancellation of the triple- Γ terms. Analytically we can be sure of exact constraint propagation only if the Bianchi identities are satisfied exactly, and that is not the case in a general coordinate basis. On the other hand, the fact that the method does work in a local Riemann normal system, and has some attractive properties of a finite differential calculus, are encouraging. Furthermore, most of the time-dependent derivatives of \mathbf{g} do cancel in the general case, and this should enhance stability. Analytical investigation of the stability of this method is difficult, so we have chosen to do so numerically.

Two numerical implementations of this scheme are being developed currently. The first assumes symmetries in two spatial dimensions, rendering the scheme explicit and avoiding the need for iteration. The second is a full implementation using staggered grids in four dimensions. Results of these studies will help in determining the stability of the method.

At best, the method is expected to be conditionally stable. The Evans-Hawley and Yee methods have this property, and are subject to a Courant-like condition on the time step (De Raedt *et al.* 2002). With $c = 1$, this implies $\Delta t < \Delta x$, which a typical condition applied in most numerical relativity implementations.

If it can be shown that such techniques provide stable constraint transport for finite difference implementations of numerical relativity, then other implementations might benefit from similar schemes that use four-dimensional grids and that have temporal and spatial derivatives that commute. In the finite element case, this would begin by extending the elements into the time direction, rather than simply time-stepping a three-dimensional finite element grid. However, some additional features would have to be introduced, analogous to grid staggering, to ensure commutation of spatial and time derivatives across element boundaries.

The pseudo-spectral may be intractable at the present time. As spatial derivatives are computed using the full spatial extent of the grid, in order to create a method in which these commuted with time derivatives, one could imagine using many, if not all, previous and future time hypersurfaces to compute the latter. This would be a truly four-dimensional grid method and involve solving the entire spacetime structure in one giant iterative procedure. Present-day computers still struggle with three-dimensional explicit schemes, so a four-dimensional implicit one is clearly beyond current technology. However, in the not-too-distant future such codes might begin to be

feasible.

The author has benefited greatly from discussions with F. Estabrook, L. Lindblom, M. Miller, D. Murphy, and M. Scheel. He is also grateful for a JPL Institutional Research and Development grant, and for the continued hospitality of the TAPIR group at Caltech. This research was performed at the Jet Propulsion Laboratory, California Institute of Technology, under contract to the National Aeronautics and Space Administration.

REFERENCES

- Clarke, D. A. 1996, *ApJ*, 457, 291–320.
- De Raedt, H., Kole, J. S., Michielsen, K. F. L., & Figge, M. T. 2002, arXiv:physics/0210035.
- Evans, C. R. & Hawley, J. F. 1988, *ApJ*, 332, 659–677.
- Stone, J. M. & Norman, M. L. 1992a, *ApJS*, 80, 753–790.
- Stone, J. M. & Norman, M. L. 1992b, *ApJS*, 80, 791–818.
- Scheel, M. A., Kidder, L. E., Lindblom, L., Pfeiffer, H. P., & Teukolsky, S. A. 2002, *Phys. Rev. D*, 66, 124005.
- Yee, K. S. 1966, *IEEE Transactions on Antennas and Propagation*, 14, 302–307.